Temperature-Dependent Lifetimes and Quantum Yield of the Singlet and Triplet States of the B820 Subunit of LHI Antenna Complex of Purple Bacterium *Rhodospirillum rubrum*

Vesa Helenius,*,† René Monshouwer, and Rienk van Grondelle

Department of Physics and Astronomy, Free University of Amsterdam, De Boelelaan 1081, 1081 HV Amsterdam, The Netherlands

Received: June 19, 1997; In Final Form: October 2, 1997[⊗]

The quantum yield and lifetimes of fluorescence and triplet state of the B820 subunit of core antenna of photosynthetic purple bacterium *Rhodospirillum rubrum* are reported at temperature range from 4.2 to 300K. The fluorescence quantum yield of B820 is strongly dependent on temperature. From 4.2 to about 200 K the yield remains nearly constant. A nonradiative decay process becomes activated around 170−200 K. Between 200 K and room temperature the quantum yield drops by a factor of 4. The fluorescence lifetimes and the B820 triplet yield follow the same temperature dependence as the fluorescence quantum yield. It is concluded that a change in the rate of internal conversion from the excited singlet state to the ground state produces the observed change. The change is modeled by using the energy gap law in the strong coupling limit. An activation energy of 65 kJ/mol and average frequency of 450 cm^{-1} for the promoting vibrational mode of the nonradiative decay are found by fitting the data by energy gap law expression. The results are compared with the bacterial reaction center and the intact bacterial light harvesting antenna. A change in the rigidity of the structure of the B820 unit induced by the isolation procedure is the probable reason for the strong temperature dependence.

1. Introduction

Initial process of both bacterial and green plant photosynthesis is the absorption of solar energy by pigment molecules in a light harvesting antenna and the transfer of the excitation energy to the reaction center.[1−4] During past decade major steps have been taken in the research of the early events of bacterial photosynthesis. These include isolation and purification of some important components of the photosynthetic machinery, e.g., a subunit of the core antenna of photosynthetic purple bacteria[5] and several bacterial reaction centers.[6−9] The crystal structures of bacterial reaction center of a purple bacteria *Rhodopseudomonas (Rps.) viridis*[10] and *Rhodobacter (Rh.) sphaeroides*[11] have been determined in atomic detail. The structure of pigment−protein complexes that are a part of the light harvesting antenna (LH-II) of *Rhodopseudomonas acidophila*[12] and *Rhodospirillum (Rs.) molishianum*[13] have become available more recently. These achievements have created a great interest in the physics of light capture and energy transfer and trapping in photosynthetic systems.

All photosynthetic bacteria contain a light harvesting antenna, which is used to increase the light absorption cross section and transfer the excitation to the reaction center (RC). The light harvesting antenna consists of pigments that are noncovalently bound to proteins. In the RC the excitation energy is used to drive an electron-transfer reaction. Both the antenna and RC of purple non-sulfur bacteria are associated with the intracytoplasmic membrane. A core antenna complex LHI that is in close contact with the RC is present in all species. Many species (e.g. *Rhodobacter sphaeroides*) also contain an additional peripheral antenna LHII.[1]

In bacteriochlorophyll *a* (BChl *a*) containing bacteria the near-infrared absorption of the LHI antenna is around 870 nm; the exact wavelength depends on the species. The LHII absorption has two peaks around 850 and 800 nm. Biochemically the LHI and LHII are very similar. The basic unit of the antenna complexes is a pair of membrane spanning helical polypeptides α and β (each about 6 kDa[14]) that bind one BChl each (B850 in LHII, B870 in LHI) to a conserved histidine residue located in the hydrophobic transmembrane section of the polypeptide. In LHII the β-peptide binds an additional BChl (B800). Carotenoids are present in a 1:1 or 1:2 ratio to BChl.[15]

The crystal structure of LHII antenna complex of *Rps. acidophila* and *Rs. molishianum* have recently become available. The crystallized LHII consists of eight (*Rs. molishianum)* or nine (*Rps. acidophila)* α,β-polypeptide pairs in a cylindrical arrangement where the α-polypeptides form the inner part of the cylinder and β-peptides are located on outer side.[12,13] The B850 pigments are enclosed between the α,β-pairs. The inner radius of LHII cylinder is 14−18 Å in diameter. LHI is believed to be very similar in arrangement[14] except larger in size because the RC has to fit in the hollow center of the cylinder. A low resolution image of a 2-dimensional crystal of purified LHI of *Rhodospirillum rubrum* (*Rs. rubrum)* gave a ring with 16 α,β-heterodimers.[16]

The light harvesting antenna of purple bacterium *Rs. rubrum* consists of a core antenna (LHI) only. The near-infrared absorption of the core antenna LHI is around 875 nm (B875). The core complex can be broken into B820 subunits (absorbing at 820 nm) by using detergents (e.g. *n*-octyl-β-D-glucopyranoside).[17] The subunit B820 represents an intermediate form between the LHI core complex and monomeric BChl *a* (absorbing at 777 nm). The formation B820 unit is very sensitive to the amount of detergent and the B875 can reversibly be reconstituted by reducing the detergent concentration. Spectroscopic evidence has indicated that the subunit B820 consists of α and β polypeptides and two molecules of BChl *a* (α,β-BChl a_2).[18,19] We have successfully used the B820 dimer as a basic element in describing energy transfer and hopping in the LHI antenna of photosynthetic purple bacteria.[20−22] For this reason it is essential to characterize the biophysical properties of the dimer in detail.

† Present address: Department of Chemistry, University of Jyväskylä, P.O. Box 35, 40351 Finland. E-mail: vesa.helenius@jyu.fi.

⊗ Abstract published in *Advance ACS Abstracts,* November 15, 1997.

S1089-5647(97)02013-0 CCC: $14.00

In this paper we report the temperature dependence of the B820 fluorescence spectrum, quantum yield, and lifetimes. Also reported are the triplet−singlet (T−S) spectrum, its temperature dependence, triplet lifetimes, and relative quantum yield as a function of temperature. In contrast to a nearly temperature independent fluorescence lifetime of LHI the B820 subunit shows strongly temperature-dependent lifetimes. The results are compared with the properties of intact LHI and LHII of *Rb. sphaeroides*. Also a comparison is made between the mechanism of internal conversion in the special pair of a bacterial RC and the B820 particle. The temperature dependence of the fluorescence quantum yield of B820 is fitted by applying the energy gap law of nonradiative decay processes.[23,24]

2. Experimental Section

The B820 subunit of *Rs. rubrum* in a 50 mM phosphate buffer containing 1% of *n*-octyl-*β*-glucopyranoside was prepared as described elsewhere.[17] The samples were stored in dark at −20 °C. For optical measurements the standard buffer was diluted in 60% (wt/wt) glycerol, 50 mM phosphate buffer (pH 7.8) and 1.15 wt %/wt detergent *n*-octyl-*β*-glucopyranoside (OG). The sample preparation was critically dependent on the amount of detergent; 1.17% of OG instead of 1.15% resulted in a sample with large fraction of monomeric BChl *a*.

Fluorescence spectra were measured by a Chromex 500IS spectrograph and a Chromspec CCD detection (1.3 nm bandwidth). An OD^{820} of 0.1/cm was used. The excitation source was a Ti:sapphire laser tuned for direct excitation of the 820 absorption band. Excitation intensity was about 2 mW/cm^2. This excitation intensity was high enough to burn holes (5% increase in transmission in 15 min at 4K) in the absorption band at low temperatures (between 4 and 50K). To compensate for the hole burning the changes in the OD were followed by measuring the changes in transmission of the exciting laser beam. The original OD could be restored by annealing to 100 K and cooling cycle. The fluorescence was detected in magic angle polarization. Oxford and Utreks liquid helium cryostats were used for the low-temperature work.

Time-resolved fluorescence was measured by time-correlated single photon counting. A part from a femtosecond white light continuum was selected by a narrow band interference filter (at 812 nm) for excitation. The white light continuum was produced by focusing the 800 nm output of a Coherent regenerative Ti:sapphire amplifier to a sapphire plate. The laser was operating at 250 kHz repetition rate. The excitation intensity at the sample was about 0.05 mW. The detection wavelength was selected a by long-pass filter at 830 nm and an interference filter at 840 nm. A magic angle polarization was used. The detection was done by a Hamamatsu R1654U multichannel plate photomultiplier (12 μm channels). An effective count rate less than 1% of the laser repetition rate was used (taking into account the dead time of the instrument). By using Ortec time to amplitude converter, Tennelec constant fraction discriminator and a Silena A/D converter a 90 ps fwhm of the instrumental response was obtained.

The flash-photolysis setup for measuring the triplet−singlet spectra and triplet lifetimes was based on a Quanta Ray PDL2 dye laser pumped by a Q-switched Quanta Ray DCR2A Nd:YAG laser at 0.5 Hz. A halogen lamp (Oriel) was used as a light source for detection. The light passing through the sample was focused on the input slit (1 nm bandwidth) of an Oriel $^1/_4$-m monochromator. The data from a fast photodiode was digitized by a LeCroy 9310 300 MHz oscilloscope. A laser flash wavelength of 585 nm was selected because of a temperature-independent OD of the B820 preparation at this particular wavelength. A homogeneous illumination of the sample was ensured by placing a diffuser on the input window of the cryostat. The sample was kept in N_2-atmosphere in a 3−4 mm thick acrylic cuvette with a 10 mm path length for measuring light. All the measurements were done at laser power where bleaching of B820 absorption was linearly dependent on the power. Typical bleach was 3% of the OD at the absorption maximum.

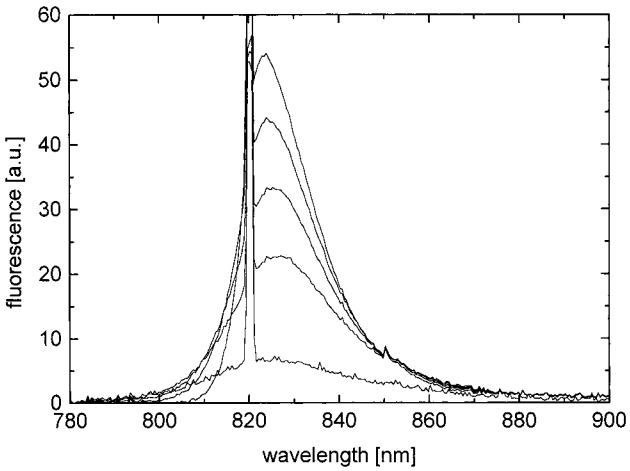

Figure 1. Fluorescence spectra of B820 at 77 K (upper curve), 180 K, 210 K, 250 K, and 298 K. Excitation wavelength is 819 nm.

3. Results

The fluorescence spectrum of the B820 subunit from the LHI antenna of *Rs. rubrum* peaks at 826 nm (4 K) when excited at 819 nm. The Stokes shift of fluorescence is then 107 cm^{-1}. At higher temperatures the fluorescence maximum gradually shifts 3 nm to the blue. The fluorescence spectrum shows no vibrational structure even at 4 K when excited at 819 nm. The integrated fluorescence intensity of B820 shows a strong temperature dependence between 150 and 300 K. At low temperatures the fluorescence intensity is nearly constant. Around 200 K the fluorescence intensity starts to decrease rapidly. Figure 1. shows the fluorescence spectra of B820 from 77 to 298 K. The main features of the B820 fluorescence spectrum as a function of temperature are the broadening on the short wavelength side and a drop in fluorescence intensity. The absorption spectrum of the B820 subunit reflects the broadening observed in the fluorescence. At low temperature (77 K) the absorption spectrum of B820 is narrow (fwhm 320 nm) and about 5 nm red-shifted compared to room-temperature spectrum. Most of the spectral change takes place in the temperature range between 298 and 200 K.[25] The B820 absorption spectrum does not indicate any structural change or dissociation of the complex that might be associated with the drop in fluorescence quantum yield. The absolute quantum yield of B820 in glycerol buffer at room temperature has been determined to be 3%.[26] The 3% fluorescence quantum yield at room temperature results in 11% quantum yield at 4.2 K because our relative measurement shows an increase of the fluoresecence yield by a factor of 3.7 from *RT* to 4.2 K.

Figure 2 presents the fluorescence decay of B820 at 4.2 and 292 K obtained by single photon counting. The excitation wavelength is 812 nm, and detection is at 840 nm. The instrumental response and the fitted exponential decays are also shown. Table 1 reports the lifetimes at a range of temperatures obtained by iterative convolution. The fluorescence lifetime increases by a factor of 4.2 between *RT* and 4.2 K. This is very close to the 3.7-fold increase in the fluorescence quantum

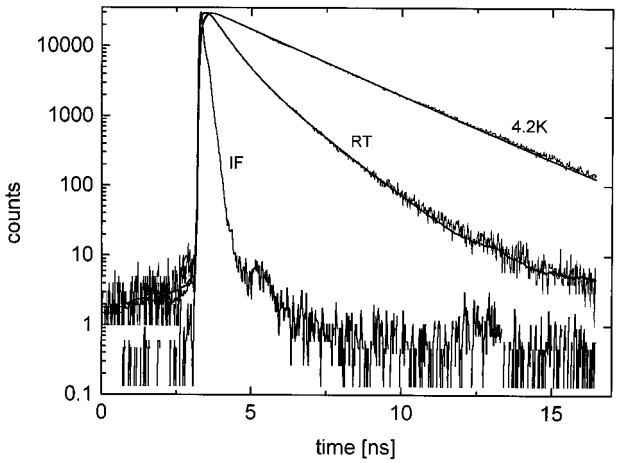

Figure 2. Fluorescence decay of B820 at *RT* and 4.2 K obtained by single photon counting. Excitation wavelength 812 nm, detection 840 nm. Instrumental response (IF) and the exponential fit to the decay are also shown.

TABLE 1: Fluorescence Lifetimes of B820 of *Rs. rubrum*

T [K]	τ_1 [ns]	τ_2 [ns]	T [K]	τ_1 [ns]	τ_2 [ns]
4.2	2.29		120	2.22	
40	2.27		200	2.12	
77	2.25		298	0.55 (74%)	1.30 (26%)

[a] Excitation at 812 nm, detection at 840 nm. Amplitudes in parentheses.

yield taking into account that the fluorescence lifetimes vary slightly between different preparations (from 2.44 to 2.25 ns at 77 K). We suggest that the lifetime is dependent on the detergent and glycerol concentration. This agrees with the observation of Chang et al.[27] that the fluorescence yield of monomeric BChl *a* decreases with decreasing OG concentration.

At room temperature two distinct lifetimes are observed. The longer 1.3 ns lifetime (26% preexponential factor) component is assigned to monomeric BChl *a*. Our preparations contained variable amount of dissociated pigment complex B777 (less than 10% compared to B820 absorption). At room temperature the excitation between 800 and 812 nm excites the red edge of the B777 absorption band. Because B777 has a higher quantum yield than B820 the fluorescence of B777 has relatively large contribution even at 840 nm. At low temperatures (<200 K) the absorption bands are narrower and the observed fluorescence is only due to B820.

To achieve a full picture of the excited-state decay of B820 unit the temperature dependence of the B820 triplet−singlet (T−S) spectrum, lifetimes, and relative quantum yield were also recorded. Figure 3 shows the ΔOD spectrum of B820 at 77 K after a 5 ns-laser flash at 585 nm. The spectrum is characterized by a strong bleaching around 825 nm and an induced absorption at 796 nm. The spectrum corresponds to the one reported by Van Mourik et al.[19] except for the maximum of the induced absorption. In our case it is 5 nm to the blue from the value reported previously. We think that this difference can partly be explained by the variable amount of residual "monomeric" BChl *a* in the preparation. The other reason for the difference between the spectra can be excitation wavelength that was 605 nm in the study of Van Mourik et al. The weak bleaching at 770 nm and excited sate absorption around 700 nm are caused by the nonselective excitation at 585 nm. They are not due to B820 as Van Mourik et al.[19] showed by selective excitation of B820 at 825 nm. Most likely these features come from the "monomeric" BChl *a* (B777). The T−S spectrum reflects the dimeric nature of B820 unit. As the triplet state is formed it is

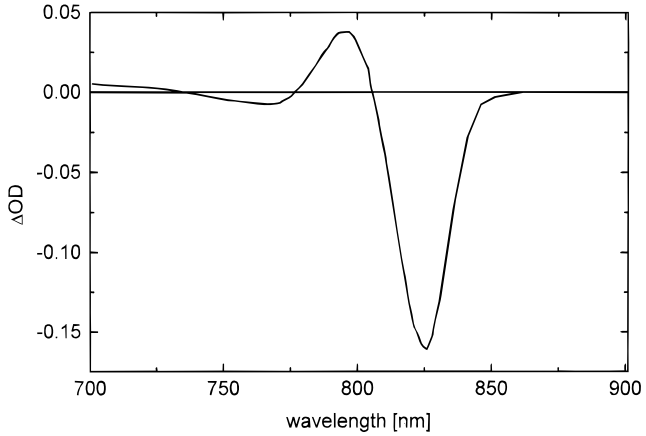

Figure 3. ΔOD spectrum of B820 unit at 77 K after a 5 ns laser flash at 585 nm.

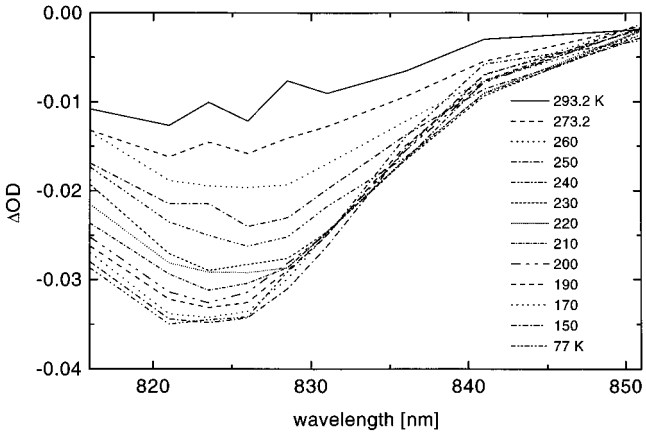

Figure 4. Temperature dependence of the ΔOD spectrum of B820 between 77 and 298 K. The ΔOD is increasing with decreasing temperature. Temperature as in Table 2.

localized to one of the BChl's of the B820 pair, the exciton interaction between the BChl's is interrupted and the remaining BChl behaves then more like a monomeric molecule. Therefore the dimeric absorption band at 820 nm is bleached (the triplet state absorption is not at this spectral region), and the absorption of the remaining BChl *a* is induced around 796 nm.

The main features of the temperature-dependent T−S spectra (Figure 4) are the strong variation of the ΔOD of the bleaching of B820 and the broadening of the spectra at higher temperatures. These spectra were calculated by fitting the triplet decay trace by single exponential and extrapolating the amplitude of the decay to the time zero (the time of the arrival of the bleaching laser flash). The wavelength of the maximum absorption changes only little as a function of temperature. The blue side of the ΔOD spectrum at 820 nm is affected by the induced absorption around 795 nm making it difficult to judge whether the real bleaching maximum shows exactly the same 5 nm shift as the absorption spectrum. At the two highest temperatures 293.2 and 273.15 K a slow sample degradation was observed in repeated measurements. An irreversible photobleaching of a small (<0.003%) fraction of the B820 absorption band resulted after each laser flash. No photoproducts were detected. The amount of sample destruction was less than 0.7% during a spectral run at 293.2 K. The sample degradation could not be avoided by degassing the sample by several freeze−thaw cycles or keeping it in N_2-atmosphere. At temperatures lower than 260 K no permanent photobleaching was observed. The triplet state lifetimes change by a factor of 6 from 126 to 20 μs when going from 77 K to room temperature

TABLE 2: Lifetime of the Triplet State of the B820 Unit of *Rs. rubrum*[a]

T [K]	τ_1 [μs]	T [K]	τ_1 [μs]
77	126 ± 5	230	97
150	123	240	82
170	124	250	72
190	119	260	58
200	118	273.2	41
210	117	293.2	20
220	107		

[a] Excitation wavelength 585 nm.

TABLE 3: Nonradiative Lifetimes of the LH I and LH II Antenna of *Rb. sphaeroides*

T [K]	LH II [ns]	T [K]	LH I [ns]
4.8	1.33	4	1.32
30	1.32	50	0.99
77	1.29	100	0.77
100	1.30	150	0.70
150	1.22	200	0.65
200	1.17	250	0.60
250	1.14		
280	1.06		

(Table 2). The numbers listed in Table 2 are averaged over nine decay curves from 816 to 851 nm. The lifetimes are wavelength independent within 5 μs over this wavelength range. At 77 K an absolute triplet yield of 0.16 has been reported for B820 in comparable conditions.[19]

4. Discussion

The fluorescence quantum yield and lifetime of the B820 unit follow the same kind of pattern as a function of temperature. The most apparent explanation for this observation is that the rate of nonradiative decay is temperature dependent. This conclusion is strongly supported by a similar temperature dependence of the B820 triplet yield.

One possible explanation for the temperature dependence of the internal conversion rate of B820 is mixing in of charge transfer (CT) states. It has been observed that in the excited special pair P* of a bacterial RC the recombination of a CT-state contributes to the fast internal conversion of the special pair. At room temperature the P* decay is about 200 ps in the D_{LL} mutant of *Rhodopseudomonas capsulatus*. The decay time of the P* of a *Rhodobacter sphaeroides* mutant with Tyr M210 replaced by a Trp is also about 200 ps. This mutation dramatically slows down the charge separation. In both systems lowering the temperature to less than 100 K slows down the P* decay approximately by a factor of 5.[28,29] One argument to support the role of CT-state is the so-called heterodimer that has a pronounced CT-state according to Stark spectrum. In the heterodimer the rate of internal conversion is close to $(30\ \text{ps})^{-1}$. However, the recombination of the CT-state cannot be the mechanism of the fast internal conversion of the B820 particle. B820 has almost no Stark effect[30,31] that indicates that in the case of B820 the CT-state does not have any significant role.

A more reasonable explanation is evident when the B820 is compared with intact LHII and LHI of *Rb. sphaeroides*. In the LHII antenna the rate of nonradiative decay is about $(1\ \text{ns})^{-1}$ at *RT* and some 20% slower at 4 K. For the LHI the rate is about $(0.5\ \text{ns})^{-1}$ at *RT* and about $(0.8-1.0\ \text{ns})^{-1}$ at 4 K (Table 3, calculated from the data of Monshouwer et al.).[26] Both LHII and especially LHI have huge Stark effects, but the change in the internal conversion rate is small compared to B820. In the LHI/LHII antenna the polypeptides and the bacteriochlorophylls are tightly bound. We suggest that the isolation of the B820 particle by a detergent affects the rigidity of the α,β-polypeptide pair and makes the bonding of the bacteriochlorophyll dimer less tight. Therefore the thermally excited phonons have a much more pronounced effect on the internal conversion of the B820 than on the internal conversion of the intact LH antenna.

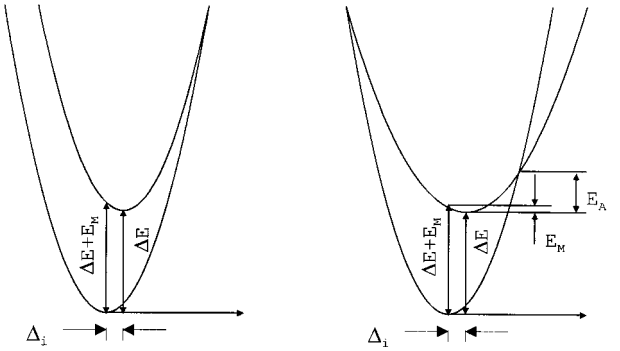

Figure 5. (a, left) Weak coupling limit of two identical harmonic vibrational potential energy surfaces. The relative displacement Δ_i between the first excited state and the ground state is small. Horizontal transitions are only allowed by tunneling mechanism. (b, right) The same as 5a, except that the excited-state potential is 50% less steep. In this case an activated transition over the energy barrier E_A is possible. (see text).

Theoretical calculation of the nonradiative decay rates in large molecules seems to be a rather challenging problem.[32] There are only few cases where expressions are available that can be used to fit the experimental data. Jortner et al.[23,33] have developed a theory for nonradiative decay processes in large molecules based on the harmonic approximation of the vibrational potentials. Their treatment describes the intramolecular nonradiative decay probability between two electronic states where the upper state consists of a small number of vibronic levels and the lower state is a dissipative continuum of vibrational levels. Analytical expressions could be obtained for two limiting cases: a weak and a strong coupling limit.

Figure 5a illustrates the weak coupling limit for two identical harmonic potential energy surfaces. The coupling is weak when the relative displacement Δ_i between the potentials is small and the crossing point for the two potentials is very high in energy. In this case the nonradiative decay rate between the two levels is exponentially dependent on the energy gap ΔE between the energy levels. The strong coupling limit corresponds to a situation where the displacement Δ_i of the potentials is large and therefore the crossing point of the potential surfaces is much lower in energy. In this case an activated decay process over the crossing point of the potentials becomes possible. If the two potential surfaces are identical the strong coupling case implies that the Stokes shift considerably exceeds the mean vibrational frequency. This is not usually observed for the fluorescence of native chlorophylls.[24] The Stokes shift of the B820 unit is about 110 cm^{-1} at 4 K. This does not indicate a very strong electron−phonon coupling. If compared to the weak and strong coupling limits of Jortner et al.[23,33] the coupling seems to be intermediate.

The weak coupling limit predicts only a weak temperature dependence of the nonradiative decay rate over the normal experimental temperature range (4.2−300 K). This happens because in the weak coupling case the promoting modes are predicted to be the high-frequency vibrations (C−H stretch at $\approx$3000 cm^{-1})[23,33] and the decay rate depends on the number of thermally excited vibrations. As the factor kT corresponds only to about 210 cm^{-1} at room temperature there is little change in the number of excited CH-modes between 4 and 300 K.

A more realistic representation of the vibrational potentials takes into account the fact that vibrational frequencies in the

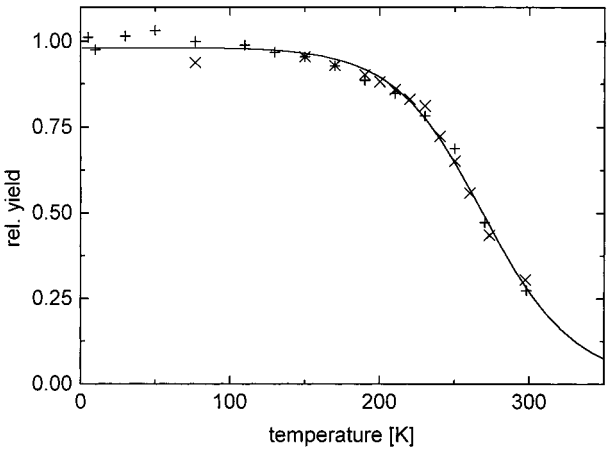

Figure 6. Measured relative fluorescence and triplet quantum yield of B820 fitted by an energy gap law expression. Fluorescence (+), triplet yield (×).

excited electronic state can be considerably lower than the ground-state frequencies. For example, for aromatic hydrocarbons the chance of some low-frequency vibrations is of the order of 50%.[32] Figure 5b shows the effect of a 50% less steep excited-state potential on the intersection of the potentials. The displacement Δ_i is the same both in part a and b of Figure 5. In this case the activation energy E_A for the barrier crossing is much smaller than in the case of two identical potentials. The strong coupling case with frequency changes has also been treated by Jortner et al.[33] Except for a constant factor it leads to a similar temperature dependence of the nonradiative decay rate as the case with identical vibrational frequencies.

Although the harmonic approximation is hardly valid for ground-state vibrational levels with excess of 15 000 cm^{-1} of energy, two important features of the nonradiative process can be recognized from the treatment of the harmonic case. When the coupling is weak, the nonradiative decay proceeds via a tunneling mechanism, leading to an exponential dependence of the decay rate on the energy gap between the ground and excited state. In the case of strong coupling or higher temperatures an activated process over an energy barrier E_A becomes possible.[32] Also a temperature-dependent transition from a weak to a strong coupling case is possible, because the coupling itself is temperature dependent.[23]

We used the "strong coupling limit" of the expression given by Jortner et al.[23] to fit the temperature dependence of the B820 fluorescence and triplet quantum yields. The temperature-dependent rate of nonradiative decay is

$$k_{nr}(T) = \frac{C}{(k_B T_{eff})^{1/2}} \exp\left(\frac{-E_A}{k_B T_{eff}}\right) \quad (1)$$

where T_{eff} is the effective temperature

$$k_B T_{eff} = {}^1/_2 \hbar\omega_m \coth(\beta\hbar\omega_m/2) \quad (2)$$

The k_{nr} is the sum of the nonradiative decay rates, C is a constant, $\beta = 1/k_B T$, and ω_m is the mean vibrational frequency of the active modes of the nonradiative decay. E_A is the activation energy for the nonradiative decay.

The simple harmonic oscillator model fits the temperature dependence of the experimental data well. An activation energy of 65 kJ/mol and an average frequency of 450 cm^{-1} for the promoting mode are found by simultaneously fitting the fluorescence and triplet data. Figure 6 shows relative fluorescence and triplet quantum yields of B820 together with a simulated curve. We feel that the model correctly describes the overall process where the rate of nonradiative decay increases with temperature due to thermally excited phonons. Because the model is highly idealized, the numerical values of the parameters should not be given too much weight. The average frequency obtained from the fit might not reflect a real vibrational frequency of the B820 unit.

The quantum yield of fluorescence and the fluorescence lifetime remain nearly constant from 4.2 to about 170−200 K where an activated decay process appears. The same process can be observed in the quantum yield of the B820 triplet state. Therefore we conclude that it is the internal conversion that becomes thermally activated around 200 K. We do not think that it has to do with a phase transition of the B820 unit nor a phase transition of the glycerol buffer because the change it the nonradiative decay rate takes place smoothly over a large temperature range. Furthermore, the optical spectra (absorption, fluorescence, or triplet spectrum) do not show any abrupt changes around 200 K. It is interesting to note that also the lifetime of the B820 triplet state depends strongly on temperature (Table 2). The change is even bigger than the change in the fluorescence lifetimes over the same temperature range.

4. Conclusion

Fluorescence quantum yield and lifetimes of the B820 subunit of the core antenna of *Rs. rubrum* are reported at temperature range from 4.2 to 300 K. The temperature dependence of the fluorescence quantum yield of B820 is strong. A nonradiative decay process is activated around 170 to 200 K. The fluorescence quantum yield is nearly constant from 4.2 to about 200 K. Between 200 K and room temperature the quantum yield drops by a factor of 4. The fluorescence lifetimes follow the same temperature dependence as the quantum yield, dropping from 2.1 ns (200 K) to 0.55 ns (298 K). The lifetime we observe at room temperature is shorter than the one observed by Chang et al.[27] (0.55 ns compared to 0.72 ns). The result presented in this paper is consistent with other measurements in our laboratory.[25] The discrepancy may be due to a difference in detergent concentration and the glycerol buffer that we used.

The temperature dependence of the B820 triplet yield shows the same behavior as the fluorescence quantum yield. Therefore we conclude that it is the rate of internal conversion from the excited singlet state to the ground state that is responsible for the observed change. The temperature dependence of the nonradiative decay of B820 is modeled by using the energy gap law in the strong coupling limit. The energy gap law based on a harmonic approximation of the vibrational potentials can successfully be used to describe the experimental results. An activation energy of 65 kJ/mol and average frequency of 450 cm^{-1} for the promoting vibrational mode of the nonradiative decay are found by fitting the data by energy gap law expression.

When the excited-state properties of the B820 particle are compared with the intact light harvesting antenna LHI or LHII a much stronger temperature dependence is observed. Our interpretation is that the isolation of the α,β-polypeptide pairs from the cell membrane changes the rigidity of (α,β-BChl a_2) packet. The low-frequency vibrations that are introduced by the change in the environment of the B820 can effectively be coupled to the phonons of the surrounding medium. The role of the charge transfer state that has been suggested for the mechanism of the decay of the P* is ruled out by the very weak Stark effect of the B820.

Acknowledgment. We thank the technical staff of the Biophysics group of the Free University of Amsterdam.

Especially Ing. Henny van Roon is acknowledged for skillful preparation of B820 stock solutions. This research was supported by the Academy of Finland, the EC contract 93-0278, the Dutch Foundation for Fundamental Research (NWO), through the Foundation of Life Sciences (SCW) and the Human Frontiers in Science Program.

References and Notes

(1) Van Grondelle R.; Dekker J. P.; Gillbro T.; Sundström V. *Biochim. Biophys. Acta* **1994**, *1187*, 1.
(2) Fleming G.; van Grondelle R. *Phys. Today* **1994**, *47*, 48.
(3) Knox R. S. In *Primary Processes of Photosynthesis*; Barber J., Ed.; Elsevier: Amsterdam. 1977; pp 55−97.
(4) Sauer K. in *Bioenergetics of Photosynthesis*; Govindjee, Ed.; Academic Press: New York, 1975; pp 115−181.
(5) Miller J. F.; Hinchigeri S. B.; Parkes-Loach P. S.; Callahan P. M.; Sprinkle J. R.; Loach P. A. *Biochemistry* **1987**, *26*, 5055.
(6) Vasmel H.; Swarthoff T.; Kramer H. J. M.; Amesz J. *Biochim. Biophys. Acta* **1983**, *725*, 361.
(7) Hurt E. C.; Hauska G. *FEBS Lett.* **1984**, *168*, 149.
(8) Trost J. T.; Blankenship R. E. *Biochemistry* **1989**, *28*, 9898.
(9) Van de Meent E. J.; Kleinherenbrink, F. A. M.; Amesz, J. *Biochim. Biophys. Acta* **1990**, *1015*, 223.
(10) Deisenhofer J.; Epp O.; Miki K.; Huber R.; Michel H. *Nature* **1985**, *318*, 618.
(11) Allen J. P.; Feher G.; Yeates T. O.; Komiya H.; Rees D. C. *Proc. Natl. Acad. Sci. U.S.A.* **1987**, *84*, 5730.
(12) McDermott, G.; Prince, S. M.; Freer, A. A.; Hawthornthwaite-Lawless, A. M.; Papiz, M. Z.; Cogdell, R. J.; Isaacs, N. W. *Nature* **1995**, *374*, 517.
(13) Koepke J.; Hu X.; Muenke C.; Schulten K.; Michel H. *Structure* **1996**, *4*, 581.
(14) Zuber, H.; Brunisholz, R. In *Chlorophylls*; Scheer H., Ed.; CRC Press: Boca Raton, FL, 1991; pp 627−703.
(15) Hawthornthwaite, A. M.; Cogdell, R. J. In *Chlorophylls*; Scheer, H., Ed.; CRC Press: Boca Raton, FL, 1991; pp 493−528.
(16) Karrasch S.; Bullough P. A.; Ghosh R. *EMBO J.* **1995**, *14*, 631.
(17) Miller, J. F.; Hinchigeri, S. B.; Parkes-Loach, P. S.; Callahan, P. M.; Sprinkle, J. R.; Riccobono, J. R.; Loach, P. A. *Biochemistry* **1987**, *26*, 5055.
(18) Visschers, R. W.; Chang, M. C.; van Mourik, F.; Parkes-Loach, P. S.; Heller, B. A.; Loach, P. A.; van Grondelle, R. *Biochemistry* **1991**, *30*, 2951.
(19) Van Mourik, F.; Van der Oord, C. J. R.; Visscher, K. J.; Parkes-Loach, P. S.; Loach, P. A.; Visschers, R. W.; van Grondelle R. *Biochim. Biophys. Acta* **1991**, *1059*, 111.
(20) Visser, H. M.; Somsen, O. J. G.; van Mourik, F.; Lin, S.; van Stokkum, I. H. M.; van Grondelle, R. *Biophys. J.* **1995**, *69*, 1083.
(21) Bradforth, S. E.; Jiminez, R.; van Mourik, F.; van Grondelle, R.; Fleming, G. R. *J. Phys. Chem.* **1995**, *99*, 16179.
(22) Visser, H. M.; Somsen, O. J. G.; van Mourik, F.; van Grondelle, R. *J. Phys. Chem.* **1996**, *100*, 18859.
(23) Englman, R.; Jortner *J. Mol. Phys.* **1970**, *18*, 145.
(24) Groot, M.-L.; Peterman, E. J. G.; van Stokkum, I. H. M.; Dekker: J. P.; van Grondelle, R. *Biophys. J.* **1995**, *68*, 281.
(25) Visschers R. W.; Van Mourik F.; Monshouwer R.; Van Grondelle R. *Biochim. Biophys. Acta* **1993**, *1141*, 238.
(26) Monshouwer, R.; Abrahamsson, M.; van Mourik, F.; van Grondelle R. *J. Phys. Chem.*, in press.
(27) Chang, M. C.; Callahan, P. C.; Parkes-Loach, P. S.; Cotton T. M.; Loach, P. A. *Biochemistry* **1990**, *29*, 421.
(28) Woodbury, N. W. and Allen, J. P. In *Anoxygenic Photosynthetic Bacteria*; Blankenship, R. E., Madigan, M. T., Bauer, C. E., Eds.; Kluwer Academic Publishers: Dordrecht, 1995; pp 527−557.
(29) Nagarajan, V.; Parson, W. W.; Davis, D. and Schenck, C. C. *Biochemistry* **1993**, *32*, 12324.
(30) Beekman, L. M. P.; Steffen, M.; van Stokkum, I. H. M.; Olsen, J. D.; Hunter, C. N.; Boxer, S. G.; van Grondelle, R. *J. Phys. Chem. B* **1997**, in press.
(31) Beekman, L. M. P.; Frese, R. N.; Fowler, G. J. S.; Picorel, R.; Cogdell, R. J.; van Stokkum, I. H. M.; Hunter, C. N.; van Grondelle, R. *J. Phys. Chem. B* **1997**, in press.
(32) Medvedev, E. S.; Osherov V. I. *Radiationless Transitions in Polyatomic Molecules*; Springer Series in Chemical Physics 57; Springer-Verlag: Berlin Heidelberg, 1995.
(33) Freed, K. F.; Jortner, J. *J. Chem. Phys.* **1970**, *52*, 6272.